Sintering kinetics of pure and doped chromium oxide

S. N. ROY, S. R. SAHA*, S. K. GUHA
Central Glass and Ceramic Research Institute, Jadavpur, Calcutta 700 032, India

The mechanism of sintering in chromium oxide in the presence of varying amounts of magnesium oxide in a firing condition that simulates a controlled reducing atmosphere has been investigated. The investigation is based on isothermal shrinkage measurements at different temperatures. The data suggest grain boundary diffusion to be the main process with evidence of vapour transport.

1. Introduction

Sintered chromium oxides as a ceramic material have proved to be useful for their excellent corrosion resistance [1] for certain types of special glasses at high temperatures. They have also been found to possess excellent thermal shock resistance property. Hagel *et al.* [2], Jorgensen [3] used argon atmospheres with a P_{O_2} of about 10^{-2} mm to study the initial sintering but were unable to obtain a high density product. Anderson [4] repeated the experiment and was also unable to sinter Cr_2O_3. Halloran and Anderson [5] studied the dependence of partial pressure of oxygen on the initial sintering of chromia and their results confirmed the data of Ownby and Jungquist [6]. Investigation [7] on sintering of Cr_2O_3 in reducing conditions by heating compacted mixtures of finely divided chromium oxide and carbon and the results emphasized the role of grain boundaries on sintering. Hench [8] concluded that both evaporation–condensation and volume diffusion were operative in sintering of Cr_2O_3 in air. Several transitional metal oxides [9, 10] was used as sintering aids but except for TiO_2, none were found to be effective. Johnson and co-workers [11–13] as well as Thummler and Thomma [14], determined kinetics of sintering, from plots of logarithm of shrinkage against logarithm of time for a sintering material.

The present investigation aims at the study of isothermal sintering kinetics of Cr_2O_3 based on isothermal shrinkage measurement in the presence of varying amounts of MgO at different temperatures. The firing conditions maintained more or less a simulated controlled reducing atmosphere with a very low P_{O_2} which was the consequence of the formation of carbon monoxide from graphite granules used around the sintering zone. From the kinetic data, the probable mechanism of mass transport has been suggested. The fractured surface of the densest specimen obtained in the present study has been examined under a scanning electron microscope (SEM) for grain growth and existence of closed pores. The same sample has also been examined with a polarizing microscope (Ortholux Pol) to show the presence of a new phase along the grain boundaries.

2. Experimental details

Chromium oxide (Cr_2O_3) used in the study was the high purity grade of Thomas Baker & Co., London (99.9% purity). The particle size distribution of the Cr_2O_3 powder determined by the Sartorius sedimentation balance is shown in Fig. 1. AR grade $Mg(NO_3)_2$ was used as the source of MgO.

For the doped samples, a weighed amount of $Mg(NO_3)_2$ was dissolved in distilled water and mixed with the preweighed Cr_2O_3. This mixture was stirred continuously with a magnetic stirrer about 6 h for homogenization. The mixture was then carefully dried. The powders were then calcined at 600° C to liberate out the NO_2 gas. The baked material was further wet ground. All samples in the form of square pellets 1.54 cm $\times$ 1.54 cm $\times$ 0.7 cm in size were obtained by applying pressure of about 122 MPa by a hydraulic press to produce a more uniform maximum green compaction density of about 3.33 g cm^{-3}. The density used to compute the per cent of theoretical density of both pure and doped material was 5.21 g cm^{-3}.

The green samples were placed between two sintered alumina substrates and the whole assembly, surrounded by graphite granules to prevent oxidation of the samples, was placed into a squat shaped sintered alumina crucible (250 ml capacity). A sintered alumina lid was used as a cover. Around the lid, a mixture of plastic clay and Al_2O_3 powder was used as the roller material. The crucible was fired at 1623, 1673, 1723 and 1773 K with soaking time ranging from 10 to 360 min in each case using a Supercanthal furnace. The rate of heating was 373 K h^{-1}. The crucible was taken out. The samples were cleaned and measured for various properties. The data reported in the paper were evaluated on the basis of two experiments.

3. Results and discussion

Kinetic parameters like *n*-value, activation energy and frequency factor calculated for different compositions studied and temperatures used for their sintering are given in Table I. Figs 2 to 7 show the plots of percentage relative shrinkage against time (min) in log–log scale of the different samples. These plots are based on

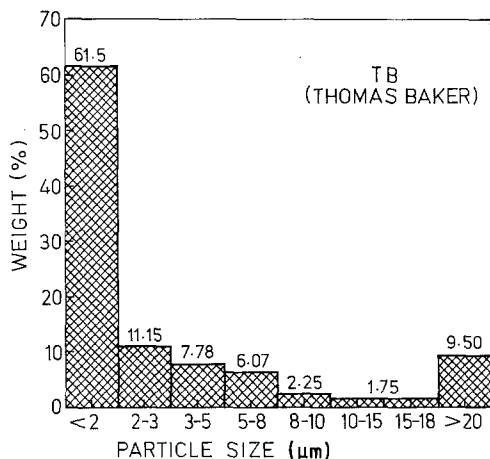*Present address:* Department of Inorganic Chemistry, Jadavpur University, Calcutta 700 032, India.

Figure 1 Distribution of particle size in chromium oxide.

the equation

$$\log\left(\frac{\Delta L}{L_0} \times 100\right) = \log K_T + n \log t \qquad (1)$$

where K_T is a temperature dependent constant, $\Delta L/L_0$ is the relative linear shrinkage, t is the time and n is an exponent whose value varies with the mechanism of material transport. n is calculated from the slope of the plot while $\Delta L/L_0$ at $t = 1$ gives K_T. Using an Arrhenius equation, plots of $-\log K_T$ against reciprocal temperature $(1/T)$ for different samples are shown in Fig. 8. Slope of these plots gives $Q/2.303R$ from which Q, the activation energy, is calculated while the intercept on $-\log K_T$ axis gives $-\log A$ from which the frequency factor A is calculated. The calculated values of n reveal that although they range between 0.1 and 0.3, they are mostly centred around 0.2. It has

been pointed out by Johnson [15] that n varies from 0.32 to 0.47 depending on the relative importance of grain boundary and volume diffusion in the material transport. Singu [16] has shown that the slope is increased by concurrent surface diffusion and decreased by vapour transport. In the present study, although the effect of MgO on the value of n in the light of foregoing findings positively indicate that the mechanism operative in the sintering of Cr_2O_3 in presence of varying amounts of MgO is predominantly a grain boundary diffusion process with concurrent vapour transport having varying contribution. Such a conclusion also follows the work of Stone [17] who has pointed out that departure of the oxide from stoichiometry with increase in lattice diffusion appears to be the most important process in sintering but the possibility of an initial vapour transport cannot be ruled out. Further, it is observed that the sintered mass obtained in this study contain black grains which can be highly polished but on pulverising, turns distinctly green. This observation is also in accord with that of Stone [17]. Lastly, the relatively low activation energy (125 to 272 kJ mol^{-1}) found for the present system is also indicative of the predominance of grain boundary diffusion although the reported activation energy for sintering of isostructural alumina by the same grain boundary diffusion is relatively higher (628 kJ mol^{-1}). It is interesting to note that log shrinkage against log time plot for each sample at different temperatures (Figs 2 to 7) are linear and nearly parallel. This indicates that a similar mechanism is operative in each case throughout the whole process and at all temperatures. The slightly higher value of n found for all the samples at the lowest

TABLE I Kinetic data for the sintering of chromium oxide in presence of different wt % of magnesium oxide

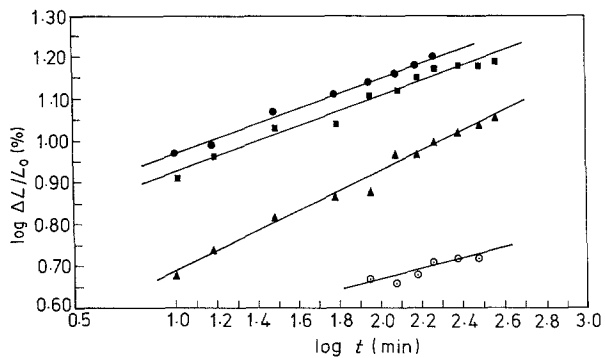| Sample No.	Composition (wt %)	Temperature (K)	Value of n	Activation energy, Q (kJ mol^{-1})	Frequency factor, $A \times 10^2$ (min^{-1})
TB$_{M-0}$	Cr_2O_3 100.00 MgO 0.00	1623 1673 1723 1773	0.13 0.24 0.18 0.18	158.654	31.52233
TB$_{M-1}$	Cr_2O_3 99.90 MgO 0.10	1623 1673 1723 1773	0.21 0.14 0.14 0.14	121.712	3.50668
TB$_{M-2}$	Cr_2O_3 99.75 MgO 0.25	1623 1673 1723 1773	0.28 0.30 0.20 0.19	200.656	566.9787
TB$_{M-3}$	Cr_2O_3 99.50 MgO 0.50	1623 1673 1723 1773	0.16 0.16 0.11 0.10	206.118	1347.18672
TB$_{M-4}$	Cr_2O_3 99.00 MgO 1.00	1623 1673 1723 1773	0.23 0.08 0.08 0.08	274.950	180111.040
TB$_{M-5}$	Cr_2O_3 98.00 MgO 2.00	1623 1673 1723 1773	0.26 0.15 0.16 0.14	223.591	3255.62812

Figure 2 Logarithm of percentage linear shrinkage against logarithm of time plot for TB_{M-0}. (O) 1623 K; (▲) 1673 K; (■) 1723 K; (●) 1773 K.
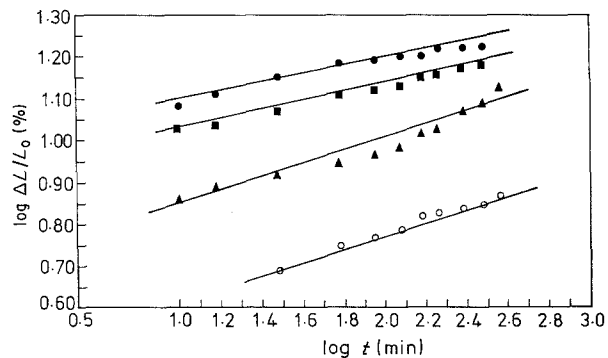

Figure 5 Logarithm of percentage linear shrinkage against logarithm of time plot for TB_{M-3}. (O) 1625 K; (▲) 1673 K; (■) 1723 K; (●) 1773 K.
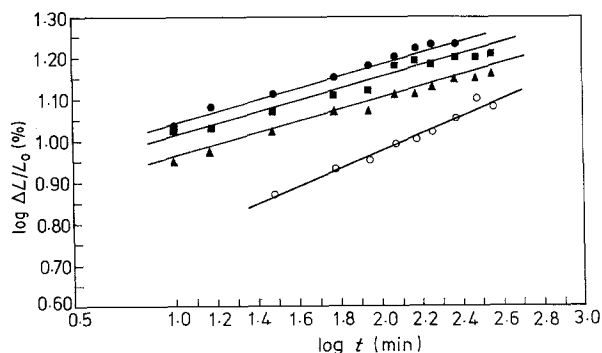

Figure 3 Logarithm of percentage linear shrinkage against logarithm of time plot for TB_{M-1}. (O) 1623 K; (▲) 1673 K; (■) 1723 K; (●) 1773 K.
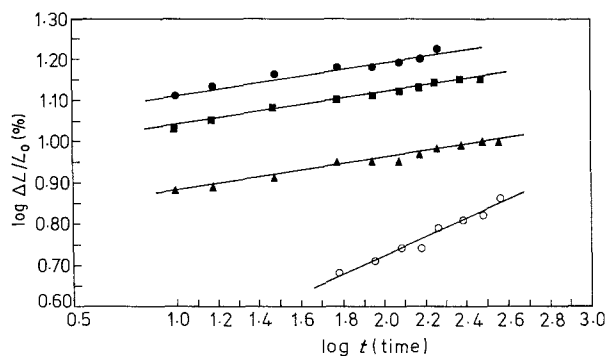

Figure 6 Logarithm of percentage linear shrinkage against logarithm of time plot for TB_{M-4}. (O) 1623 K; (▲) 1673 K; (■) 1723 K; (●) 1773 K.
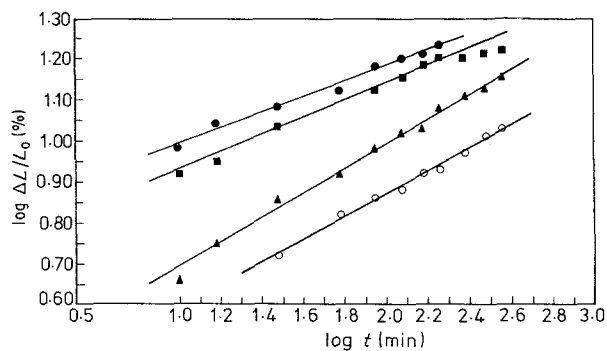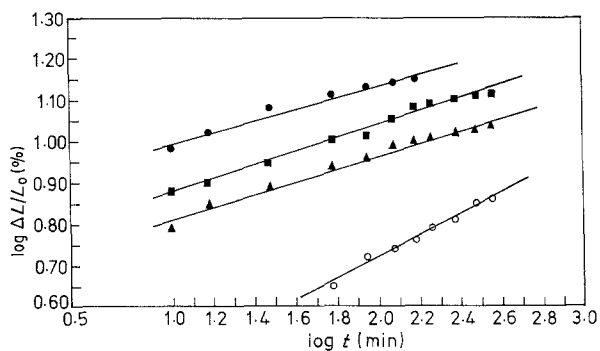

Figure 4 Logarithm of percentage linear shrinkage against logarithm of time plot for TB_{M-2}. (O) 1623 K; (▲) 6673 K; (■) 1723 K; (●) 1773 K.

Figure 7 Logarithm of percentage linear shrinkage against logarithm of time plot for TB_{M-5}. (O) 1623 K; (▲) 1673 K; (■) 1723 K; (●) 1773 K.
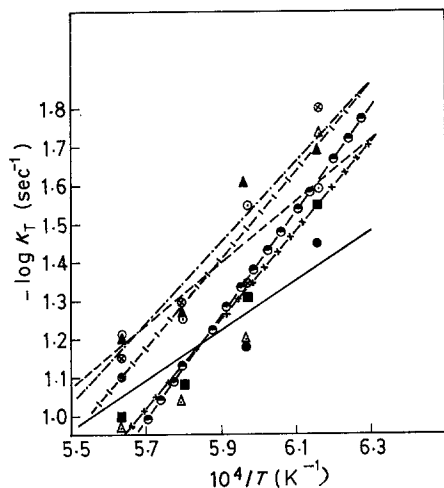
3675

Figure 8 Negative logarithm of densification rate constant against reciprocal temperature (K^{-1}) (○) TB_{M-0}; (●) TB_{M-1}; (▲) TB_{M-2}; (× ■ ×) TB_{M-3}; (⊖▲⊖) TB_{M-4}; (I⊗I) TB_{M-5}.

Figure 10 Micrograph under polarizing microscope of TB_{M-1} showing specks and strips as a new phase along the grain boundaries (×500).

temperature of study might suggest that grain boundary diffusion at that temperature predominates over vapour transport and this may be expected as reduction of Cr_2O_3 to its metal is facilitated at higher temperatures in the reducing atmosphere of carbon monoxide existing in the present system.

Maximum densification of 96% of the theoretical density, has been observed for Cr_2O_3 containing 0.1 wt % of MgO and SEM micrograph of the same (Fig. 9) shows uniform grains without any abnormal grain growth. The micrograph of the same sample taken with a polarizing microscope shows strips or specks along the grain boundaries (Fig. 10) indicating a new phase which might be magnesium chromite spinel [6]. X-ray diffraction pattern of the sample, however, reveals only Cr_2O_3 as the main phase. The hindrance to abnormal grain growth is probably associated with this spinel phase which by lying on the grain boundaries act as a barrier to grain growth.

4. Conclusions

The present study of isothermal sintering kinetics of Cr_2O_3 in presence of varying amounts of MgO indicated that sintering was predominantly a grain boundary diffusion process with simultaneous occurrence of vapour transport to varying extents and a nearly similar mechanism was operative throughout
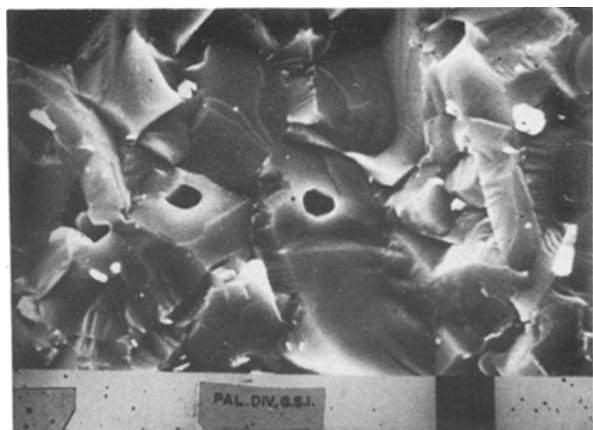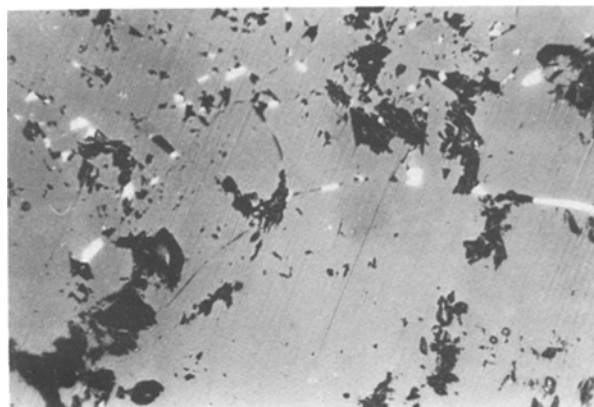
the whole process at all temperatures. The role of MgO on the kinetics was not clear but it hindered abnormal grain growth presumably forming magnesium chromite spinel on the grain boundaries.

References

1. K. L. LOWENSTEIN, in "The Manufacturing Technology of Continuous Glass Fibres" (Elsevier, New York, 1973) p. 28, 42, 67.
2. W. C. HAGEL, P. J. JORGENSEN and D. S. TOMALINE, *J. Amer. Ceram. Soc.* **49** (1966) 23.
3. P. J. JORGENSEN, private Communication (1971).
4. H. U. ANDERSON, private Communication (1971).
5. J. W. HALLORAN and H. U. ANDERSON, *J. Amer. Ceram. Soc.* **57** (1974) 150.
6. P. W. OWNBY and G. E. JUNGQUIST, *ibid.* **55** (1972) 433.
7. H. E. N. STONE and N. A. LOCKINGTON, *J. Mater. Sci.* **2** (1967) 112.
8. L. L. HENCH, PhD thesis, Ohio State University (1964).
9. W. D. CALLISTER, M. L. JOHNSON, I. V. CUTLER and R. W. URE Jr, *J. Amer. Ceram. Soc.* **62** (1979) 208.
10. S. N. ROY and S. K. GUHA, *Trans. Ind. Ceram. Soc.* **44** (1985) 49.
11. I. B. CUTLER and D. L. JOHNSON, *J. Amer. Ceram. Soc.* **48** (1963) 546.
12. D. L. JOHNSON and T. M. CLARKE, *Acta. Metall.* **12** (1964) 1173.
13. L. BERRIN and D. L. JOHNSON, in "Sintering and Related Phenomena" edited by G. C. Kuezynski, N. A. Hooton and C. F. Gibbon (Gordon and Breach, New York, 1967) p. 445.
14. F. THUMMLER and W. THOMMA, *Met. Rev.* **12** (1967) 69.
15. D. L. JOHNSON, in "Kinetics of Reactions in Ionic Systems", Vol. 4, edited by T. J. Gray and V. D. Frechette (Plenum Press, New York, 1969) p. 332.
16. P. H. SINGU, PhD thesis, North Western University (1967).
17. H. E. N. STONE, *Metallurgia* **77** (1968) 152.

Figure 9 Scanning electron micrograph of fracture surface of TB_{M-1} showing uniform grain size and closed pores (×2000).